

## Transmission of Electromagnetic Waves through Plasma Slabs

P. M. PLATZMAN AND S. J. BUCHSBAUM

*Bell Telephone Laboratories, Murray Hill, New Jersey*

(Received 24 May 1963)

The steady-state properties of circularly polarized electromagnetic waves propagating along a static magnetic field in plasmas characterized by a nonlocal conductivity are considered. The coupled Maxwell-Boltzmann equations are solved in the presence of short-range collisions for the wave which exhibits a resonance at frequencies near the electron cyclotron frequency. Expressions for the reflection and transmission of these waves for finite plasma slabs are obtained when the magnetic field is normal to the face of the slab. The expressions are explicitly evaluated and discussed for a wide range of physical parameters. The effect of temperature in the case of gaseous plasmas, and of degeneracy in the case of metals, on the transmission characteristics of the incident wave is twofold: At frequency below the cyclotron frequencies the position, width, and amplitude of the Fabry-Perot transmission resonances, which occur in plasmas characterized by a local conductivity are altered; at frequencies above the cyclotron frequencies anomalously large transmission occurs as a result of a "field-splash" type of resonance.

### I. INTRODUCTION

THE properties of electromagnetic waves propagating in a plasma along a magnetic field are of considerable interest. In many applications it is sufficient to characterize the plasma as a single component electron (or hole) gas immersed in a uniform neutralizing background of charge. The conduction electrons (or holes) in some metals are approximately described by such a simple model if the effects of band structure and ion dynamics (phonons) may be neglected. In general, the neglect of such effects implies that the frequency of the electromagnetic waves is considerably less than or much greater than interband energies; and that the wavelength of the radiation is larger than the lattice spacing and/or characteristic shielding lengths. Within this frequency range, the predictions of the electron gas model will apply to metals having a single light carrier and a roughly spherical Fermi surface. A gas plasma, on the other hand, can be described by the same model when the frequency of the electromagnetic field is much higher than characteristic ion cyclotron frequencies, but much less than ion and neutral particle excitation energies.

Cyclotron resonance experiments on gaseous plasmas,<sup>1</sup> metals,<sup>2,3</sup> and semiconductors<sup>4</sup> have proven to be extremely useful in determining the masses and relaxation times of carriers. To date, in experiments involving solids, two types of geometries have been employed: the so-called Azbel'-Kaner,<sup>5,3</sup> and the Galt<sup>2</sup> geometries. The specimen in both cases simulates a semi-infinite medium. In the Azbel'-Kaner geometry a static magnetic field parallel to the face of the sample is

used, and the reflection coefficient of normally incident radiation with polarization parallel or perpendicular to the magnetic field is measured as a function of the intensity of the magnetic field.

In the Galt geometry,<sup>2</sup> a static magnetic field perpendicular to the surface of the sample is utilized, and the reflection of circularly polarized waves propagating along the magnetic field is measured as a function of the applied magnetic field. This method was used extensively for bismuth under so-called "classical skin-effect" conditions, that is, where the current is a local function of the electric field. It is known that nonlocal effects (effects due to the finite velocity of the electrons) will modify the propagation characteristics of circularly polarized waves propagating along a magnetic field and that these modifications will be largest at frequencies near the cyclotron frequencies of the carriers. The effect of finite carrier velocity was first investigated by numerous authors interested in the initial value problem.<sup>6-8</sup> Recently, several authors<sup>9,10</sup> have examined the steady-state boundary value problem for a semi-infinite plasma. The conclusions of both groups were that nonlocal effects produce two basic changes in the propagation characteristics: a shift in the cyclotron resonance frequency (Doppler shift) and an additional damping (Landau, or resonance, damping).

In this paper we will be concerned with the effect of finite random velocity of the carriers on the transmission characteristics of transverse waves incident on thin electron-gas slabs. The finite velocity of the carriers arises from thermal motion for the case of gaseous plasmas and from the degeneracy of the fermions (electrons) in metals at zero temperature. We will refer to these finite velocity effects as finite temperature effects, where the temperature characterizing the metal is a de-

<sup>1</sup> J. L. Hirshfield and S. C. Brown, *J. Appl. Phys.* **29**, 1749 (1958).

<sup>2</sup> J. K. Galt, W. A. Yager, F. R. Merritt, B. B. Cetlin, and A. D. Brailsford, *Phys. Rev.* **114**, 1396 (1959).

<sup>3</sup> A. F. Kir, D. N. Langenberg, and T. W. Moore, *Phys. Rev.* **124**, 359 (1961).

<sup>4</sup> B. Lax, J. G. Mavroides, in *Solid State Physics*, edited by F. Seitz and D. Turnbull (Academic Press Inc., New York, 1960), Vol. XI, p. 261.

<sup>5</sup> M. Ia. Azbel' and E. A. Kaner, *Zh. Eksperim. i Teor. Fiz.* **30**, 811 (1956) [translation: *Soviet Phys.—JETP* **3**, 772 (1956)].

<sup>6</sup> A. G. Sitenko and K. N. Stepanov, *Zh. Eksperim. i Teor. Fiz.* **31**, 642 (1956) [translation: *Soviet Phys.—JETP* **4**, 512 (1957)].

<sup>7</sup> T. Pradham, *Phys. Rev.* **107**, 1222 (1957).

<sup>8</sup> I. B. Bernstein, *Phys. Rev.* **109**, 10 (1958).

<sup>9</sup> P. B. Miller and R. R. Haering, *Phys. Rev.* **128**, 126 (1962).

<sup>10</sup> P. M. Platzman and S. J. Buchsbaum, *Phys. Rev.* **128**, 1004 (1962); hereafter referred to as I.

generacy temperature ( $kT_F = \text{Fermi energy}$ ). We were motivated to investigate this problem by a number of recent experiments<sup>11,12</sup> on microwave transmission through thin slabs of bismuth, indium antimonide, and antimony.

In Sec. II, the solution of the coupled Maxwell-Boltzmann equations in the presence of two boundaries is reduced to the solution of a problem in an infinite but periodic medium. This "equivalent infinite-medium problem" is then solved using a Fourier series expansion of the fields. The method of solution is similar to that used by Gould<sup>13</sup> and others<sup>14</sup> in the plasma-capacitor problem. In Sec. III, we explicitly evaluate the expressions for the transmission coefficients for a wide range of physical parameters.

The transmission through a dielectric slab will exhibit a series of geometric or Fabry-Perot type of resonances when the slab thickness  $L$  is an integral number of half-wavelengths. We will show that for frequencies below the cyclotron frequency the effect of temperature is to shift these resonances, to decrease their amplitude, and (to a lesser extent) to broaden them. We will also show that for frequencies above the cyclotron frequency, the effect of temperature is to greatly (seven to eight orders of magnitude) enhance the amount of transmitted power and to produce a single large "field-splash" type of resonance in this power plotted as a function of slab thickness.

## II. SOLUTION OF THE COUPLED MAXWELL-BOLTZMANN EQUATIONS

Consider a one-component electron gas uniformly filling the space bounded by the planes  $z=0$  and  $z=L$ . The electron gas is immersed in a uniform static magnetic field  $\mathbf{B}_0$  oriented in the positive  $z$  direction. We wish to compute the reflection and penetration properties of a transverse, circularly-polarized wave normally incident from the left. Without loss of generality, we assume that the wave has a monochromatic time dependence and is of the form  $\mathbf{E} = \mathbf{E}(z)e^{-i\omega t}$ .

In general, as a result of the random velocity of the electrons, the plasma conductivity is a nonlocal integral operator. That is to say, a field with a  $\beta$  component at some point  $\mathbf{r}'$  in the plasma produces a current with an  $\alpha$  component at another point  $\mathbf{r}$  in the plasma with magnitude  $\sigma_{\alpha\beta}(\mathbf{r}, \mathbf{r}', \omega)E_{\beta}(\mathbf{r}')$ ,

$$J_{\alpha}(\mathbf{r}, \omega) = \int \sigma_{\alpha\beta}(\mathbf{r}, \mathbf{r}', \omega)E_{\beta}(\mathbf{r}')d\mathbf{r}'. \quad (1)$$

The fact that the relation between current and field is an integral one complicates the solution of the boundary value problem. In the presence of boundaries  $\sigma_{\alpha\beta}(\mathbf{r}, \mathbf{r}', \omega)$ ,

in general, is a function of the vectors  $\mathbf{r}, \mathbf{r}'$  separately, and the integral in Eq. (1) extends only over a bounded region. The exact functional dependence of  $\sigma_{\alpha\beta}$  will be determined by the geometry of the medium, the nature of the electron trajectories on impact with the boundary, and on the configuration of the external fields. Under such conditions Fourier transform methods do not simplify the analysis. However, if the electrons are specularly reflected from the bounding surfaces and if the magnetic field is normal to the boundary, then, and only then, we will show that the finite medium problem is equivalent to an infinite medium excited by a periodic array (with period  $2L$ ) of current sheets (see Fig. 1). In this "equivalent infinite-medium problem" the electric field is even and the rf magnetic field odd about the planes  $z=0, L, 2L, \dots$ .

Once the equivalence between the two problems is established, the boundary value problem is easily solved. The "equivalent infinite medium" is translationally invariant; in it the conductivity  $\sigma_{\alpha\beta}(\mathbf{r}, \mathbf{r}', \omega)$  depends only on the difference of vectors  $\mathbf{r}$  and  $\mathbf{r}'$  and the integral in Eq. (1) extends over all space. In this case, the integral relation Eq. (1) becomes an algebraic relation in Fourier space. That is to say,

$$J_{\alpha}(k, \omega) = \sigma_{\alpha\beta}(k, \omega)E_{\beta}(k).$$

The solution of the "boundary-value problem" is uniquely specified by the values of the rf magnetic field at the bounding planes  $z=0$  and  $z=L$  and by the wave equation satisfied by the electric field in the region  $0 < z < L$ . The strength of the current sheets at the planes  $z=0$  and  $z=L$  in the equivalent infinite medium are fixed to give the correct values of the rf magnetic field at the "boundary-value problem." Since it is sufficient to express all results in terms of the unknown strength of the rf magnetic field at the plane  $z=0$  (a simple scaling factor), we need only a single condition on the fields to determine the strength of the current sheet at the plane  $z=L$ . This condition is supplied by the requirement that there exist only an outgoing wave at this surface. This fixes the ratio  $E(L_-)/H(L_-)$  in the "boundary-value problem" to be equal to  $(\mu_0/\epsilon_0)^{1/2}$ , the impedance of free space. The subscript on  $L$  indicates

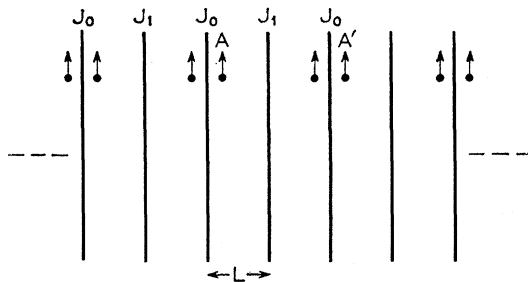


FIG. 1. The equivalent infinite medium with current sheets  $J_0$  at the planes  $(2n)L$  and current sheets  $J_1$  at the planes  $(2n+1)L$ , where  $n$  is an arbitrary positive or negative integer.

<sup>11</sup> G. A. Williams, Bull. Am. Phys. Soc. 8, 205, 353 (1963); J. Kirsch, *ibid.* 8, 205 (1963).

<sup>12</sup> A. Libchaber and R. Veilex, Phys. Rev. 127, 774 (1963).

<sup>13</sup> R. W. Gould, Bull. Am. Phys. Soc. 8, 170 (1963).

<sup>14</sup> F. L. Shure, Bull. Am. Phys. Soc. 8, 17 (1963).

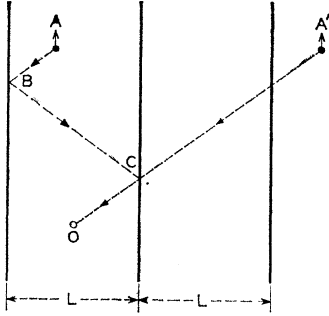


FIG. 2. Plot showing the equivalence of the path  $ABCO$  in the boundary value problem with the path  $A'CO$  in the equivalent infinite medium problem.

that the ratio  $E(z)/H(z)$  is to be evaluated as  $z \rightarrow L$  from below.

Consider an applied delta-function field at the point  $A$  (Fig. 2) in the "boundary-value problem." The equivalent field (the field which is equal to this localized field on the interval  $0 < z < L$ ) in the "equivalent infinite-medium problem" is a symmetric periodic array of delta functions (see Fig. 1). Also, there is a one-to-one correspondence between paths involving some number of reflections in the finite medium and a direct path in the periodic equivalent infinite medium. To see this, consider the contribution to the current at the point  $O$  from electrons which start out with velocity  $\mathbf{v}$  at point  $A'$  in the infinite medium. Their contribution to the current in the finite slab is zero. However, when the magnetic field is perpendicular to the surface and specular reflection exists, electrons starting out from point  $A$  with velocity  $\mathbf{v}$  and following the path  $ABCO$  give an equivalent contribution to the current. Thus, the equivalence between the currents is established for this special geometry.

The rf magnetic fields in the equivalent infinite medium are equal, by construction, to those in the finite medium. The electric field satisfies the same wave equation for the region  $0 < z < L$ , since the current induced in both media for equivalent fields are identical. We then conclude from the uniqueness of the problem that the solutions to the two problems are identical on the range  $0 < z < L$ .

For the equivalent infinite medium, and for a right-handed, circularly polarized wave [ $E_r \equiv E_x + iE_y$ ], we must solve the scalar "Helmholtz-like" equation,

$$\frac{\partial^2 E(z)}{\partial z^2} + \omega^2 \mu_0 \epsilon_0 E(z) + \frac{\mu_0}{i\omega} \int_{-\infty}^{+\infty} \sigma(z-z', \omega) E(z') dz' = i\omega \mu_0 J_s(z), \quad (2)$$

where

$$J_s(z) = -\frac{1}{\pi} \left\{ \sum_{n=-\infty}^{+\infty} H(0_+) \delta(z-2nL) + H(L_+) \delta[z-(2n+1)L] \right\}. \quad (3)$$

The field  $E(z)$  and the current  $J_s(z)$  are conveniently

represented by infinite Fourier series;

$$E(z) = \sum_{n=0}^{+\infty} a_n \cos k_n z, \quad (4)$$

$$J_s(z) = \sum_{n=0}^{+\infty} b_n \cos k_n z, \quad (5)$$

where

$$k_n = n\pi/L$$

and

$$b_n = [H(0_+) + H(L_+) \cos k_n L]/L. \quad (6)$$

$H(0_+)$  and  $H(L_+)$  are the magnitudes of the rf magnetic fields at the planes  $z=0_+$  and  $z=L_+$ , respectively. Substituting Eqs. (4) and (5) into (2) and solving for the coefficient  $a_n$ , we find

$$a_n = -\frac{i}{L} \left( \frac{\mu_0}{\epsilon_0} \right)^{1/2} k_0 [H(0_+) + H(L_+) \cos k_n L] \times \frac{[2 - \delta_{n0}]}{[k_n^2 - k_0^2 \epsilon(k_n, \omega)]}, \quad (7)$$

where  $k_0 = \omega/c$ . The quantity  $\epsilon(k, \omega) \equiv 1 + i\sigma(k, \omega)/\omega\epsilon_0$  is the relative dielectric constant of the medium,  $\sigma(k, \omega)$  is the Fourier transform of the conductivity for positive wave number  $k$ , and  $\delta_{n0}$  is the Kronecker delta.

For a right-handed circularly polarized wave, the Boltzmann equation may be linearized and solved for the scalar conductivity  $\sigma(k, \omega)$ . We find<sup>9,10</sup>

$$\sigma(k, \omega) = \frac{i\omega_p^2}{k} \int \frac{f_0 d^3v}{v_z - u}, \quad (8)$$

where

$$u = (\omega - \omega_c + i\nu_c)/k. \quad (9)$$

The quantity  $\omega_p$  is the electron plasma frequency,  $\nu_c$  is a phenomenological velocity-independent collision frequency,  $\omega_c$  is the electron cyclotron frequency, and  $f_0$  is the unperturbed electron velocity distribution function.

For a Fermi distribution with a Fermi velocity  $v_F$ ,

$$f_0 = 3/4\pi v_F^3; \quad |v| < v_F \\ = 0; \quad |v| > v_F. \quad (10)$$

Equation (8) becomes after integrating out  $v_x$  and  $v_y$

$$\sigma = \frac{i\omega_p^2}{k} \frac{3}{4v_F} \int \frac{[1 - (v_z/v_F)^2] dv_z}{v_z - u}. \quad (11)$$

For a Maxwell distribution,

$$f_0 = \frac{1}{(2\pi)^{3/2}} \left( \frac{2KT}{m} \right)^{3/2} e^{-mv^2/2KT}. \quad (12)$$

Equation (8) becomes

$$\sigma = \left( \frac{2KT}{m} \right)^{1/2} \frac{i\omega_p^2}{k} \int \frac{dv_z e^{-mv_z^2/2KT}}{v_z - u}. \quad (13)$$

The form of the conductivity in Eqs. (11) and (13) includes self-consistent field effects but does not incorporate explicit correlation effects such as exchange.

The outgoing-wave boundary condition  $E(L_-)/H(L_-) = (\mu_0/\epsilon_0)^{1/2}$  permits us to express the field  $E(z)$ , Eq. (4), in terms of  $H(0_+)$  alone. That is to say,

$$E(z) = \left( \frac{\mu_0}{\epsilon_0} \right)^{1/2} H(0_+) \left\{ f(z, L) + \frac{1}{2} \frac{H(L_+)}{H(0_+)} \times [f(L-z, L) + f(L+z, L)] \right\}, \quad (14)$$

where

$$f(z, L) = -\frac{2i}{L} \sum_{n=0}^{\infty} \frac{[2 - \delta_{n0}] \cos k_n z}{[k_n^2 - k_0^2 \epsilon(k_n, \omega)]} \quad (15)$$

and

$$\frac{H(L_+)}{H(0_+)} = -\frac{f(L, L)}{1 + f(0, L)}. \quad (16)$$

The form of Eq. (15) is particularly revealing;  $E(z)$  is generated by three terms. The first arises from the current at the plane  $z=0$ ; the other two terms result from the symmetrically placed image currents at the planes  $\pm L$ . In the limit  $L \rightarrow \infty$ , the last two terms vanish (i.e., the images recede to infinity). The summation over  $n$  then goes over into an integral, i.e.,

$$\frac{1}{L} \sum_{n=0}^{\infty} \rightarrow \frac{1}{\pi} \int_0^{+\infty} dk,$$

and the expression for  $E(z)$  becomes

$$E(z) = -\frac{1}{\pi} \left( \frac{\mu_0}{\epsilon_0} \right)^{1/2} H(0_+) k_0 \int_{-\infty}^{+\infty} \frac{e^{ikz} dk}{[k^2 - k_0^2 \epsilon(k, \omega)]}. \quad (17)$$

The expression for the impedance, the corresponding reflection coefficient, and the transmission coefficient may now be written down in terms of the functions  $f(0, L)$  and  $f(L, L)$ .

$$\frac{Z}{Z_0} = \left[ f(0, L) - \frac{f(L, L)^2}{[1 + f(L, L)]} \right], \quad (18)$$

where  $Z_0$  is the impedance of free space,

$$R = \left| \frac{1 - Z/Z_0}{1 + Z/Z_0} \right|^2 \quad (19)$$

is the fractional amount of power which is reflected, and

$$T = \left| \frac{2f(L, L)}{[1 + f^2(0, L) - f^2(L, L)]} \times \frac{Z_0}{Z} \right|^2 \quad (20)$$

is the fractional amount of incident power which is transmitted.

If the dielectric constant  $\epsilon$  is independent of  $k$  (the classical or local limit), the sums over  $k_n$  can be performed in closed form. We find, using a formula given by Knopp,<sup>15</sup> that

$$f(0, L) = i \cot(k_1 L) \epsilon^{-1/2} \quad (21)$$

and

$$f(L, L) = i [\epsilon^{1/2} \sin(k_1 L)]^{-1}, \quad (22)$$

where

$$k_1 = \epsilon^{1/2} k_0.$$

The impedance using Eq. (18) is

$$\frac{Z}{Z_0} = \frac{\cot(k_1 L) - i \epsilon^{-1/2}}{-\cot(k_1 L) + i \epsilon^{1/2}} \quad (23)$$

and the transmission coefficient is given by

$$T = |\{\cos(k_1 L) - \frac{1}{2} i \sin(k_1 L) [\epsilon^{1/2} + \epsilon^{-1/2}]\}^{-1}|^2. \quad (24)$$

These are precisely the well-known results for the impedance and transmission coefficient of a dielectric slab whose dielectric constant  $\epsilon$  is independent of  $k$ .<sup>16</sup>

### III. EVALUATION OF RESULTS

In order to evaluate Eqs. (18)–(20), some choice must be made for the equilibrium distribution function  $f_0(\mathbf{v})$ . Since this work is motivated primarily by experiments on transmission through a metal slab at low temperatures,<sup>11,12</sup> we will consider a plasma with a single, isotropic, degenerate carrier [see Eqs. (10)–(11)]. For this choice of the distribution function the dielectric constant  $\epsilon(k, \omega)$  can be evaluated in a closed form<sup>9</sup>;

$$\epsilon(k, \omega) = 1 + \frac{3}{4} \frac{\omega_p^2}{\omega k v_F} \left[ (1 - z^2) \ln \left( \frac{z-1}{z+1} \right) - 2z \right], \quad (25)$$

with

$$z = \frac{(1 - \omega_c/\omega + i\nu_c/\omega)}{(v_F/c)(k/k_0)}. \quad (26)$$

Using the above expression for the dielectric constant, Eqs. (19)–(21) were evaluated on the computer. The machine added a finite number of terms in the series defining  $f(0, L)$  and  $f(L, L)$ . A mathematical upper bound was placed on the remaining terms in the series,

<sup>15</sup> K. Knopp, *Theory and Applications of Infinite Series* (Blackie & Son Ltd., Glasgow, 1948), p. 379.

<sup>16</sup> This simple problem is identical to the problem of the reflection and penetration of particles incident on a square well potential in nonrelativistic quantum mechanics. See D. Bohm, *Quantum Theory* (Prentice-Hall, Inc., Englewood Cliffs, New Jersey, 1951), p. 243.

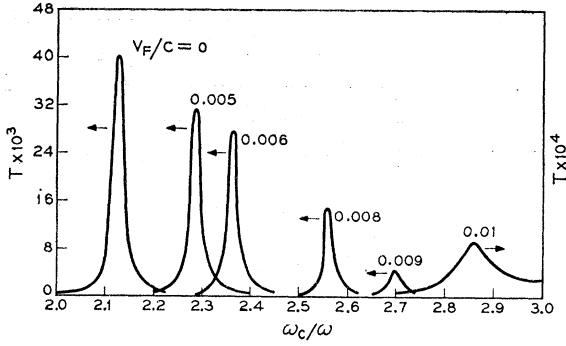


FIG. 3. Plot of the transmission coefficient  $T$  as a function of  $\omega_c/\omega$  near the  $n=3$  geometric resonance at fixed values of  $v_c/\omega = 0.01$  and  $\omega_p/\omega = 200$  for several values of  $v_F/c$ .

and the machine stopped computing terms when the fractional error in the absolute value of the remainder was found to be less than 1%. In all cases where the results could be checked exactly, the error was found to be of the order of 0.1%.

#### A. The Geometric Resonances

The transmission through a sufficiently thick dielectric slab will exhibit a series of geometric, or Fabry-Perot type, resonances as a result of the constructive interference of waves multiply scattered from the front and back plane surfaces. In a local theory, the  $n$ th-order resonance occurs when the real part of the reduced wave number  $k = n\pi/L$ , where  $n$  is an integer and where

$$k^2/k_0^2 = \epsilon(0, \omega). \quad (27)$$

The strength and width of these resonances are determined by inserting Eq. (27) into Eq. (24).

In the presence of finite temperature effects the situa-

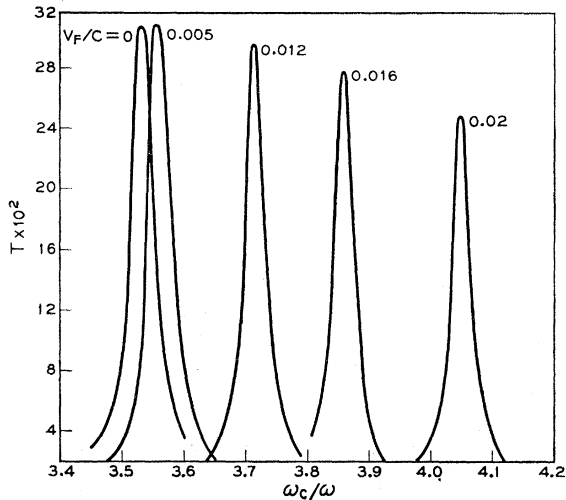


FIG. 4. Plot of the transmission coefficient  $T$  as a function of  $\omega_c/\omega$  near the  $n=2$  geometric resonance at fixed values of  $v_c/\omega = 0.01$  and  $\omega_p/\omega = 200$  for several values of  $v_F/c$ .

tion is more complicated. We have evaluated the transmission at finite temperatures for a range of various plasma parameters and have plotted representative results in Figs. 3–8. Figures 3 and 4 are plots of the transmission coefficient in the neighborhood of the  $n=3$  and  $n=2$  resonances. The plots are made as a function of magnetic field ( $\omega_c/\omega$ ) for an assumed value of  $\omega_p/\omega$  equal to 200, a fixed value of  $v_c/\omega$  equal to 0.01, and a few values of the Fermi velocity  $v_F/c$ . The effect of the finite carrier velocity is threefold. It shifts the position of the transmission resonance, it decreases its amplitude, and, to a lesser extent, it tends to broaden these resonances. In Fig. (5) are plots of the shift  $\Delta(\omega_c/\omega) \equiv (\omega_c/\omega) - (\omega_c/\omega)_{v_F/c=0}$  of the position of the resonances versus  $(v_F/c)^2$ . For both resonances  $\Delta(\omega_c/\omega)$  is proportional to  $(v_F/c)^2$  for small  $(v_F/c)$ . For larger values of  $(v_F/c)$ , the displacement of the resonance maximum increases more rapidly than  $(v_F/c)^2$ .

Consider the series expansion of Eq. (25) for large  $|z|$  or equivalently small  $(v_F/c)$ . To lowest order we find

$$\epsilon(k, \omega) = 1 - \frac{\omega_p^2}{\omega^2(1 - \omega_c/\omega + i\nu_c/\omega)} \times \left[ 1 + \frac{1}{5} \frac{k^2 v_F^2}{\omega^2(1 - \omega_c/\omega + i\nu_c/\omega)^2} \right]. \quad (28)$$

For small values of  $|(k/k_0)(v_F/c)/(1 - \omega_c/\omega + i\nu_c/\omega)|$ , the position of the resonance will be approximately determined by the solution of Eq. (28) with  $k$  set equal to  $(n\pi/L)$ . Forgetting for the moment the small imaginary

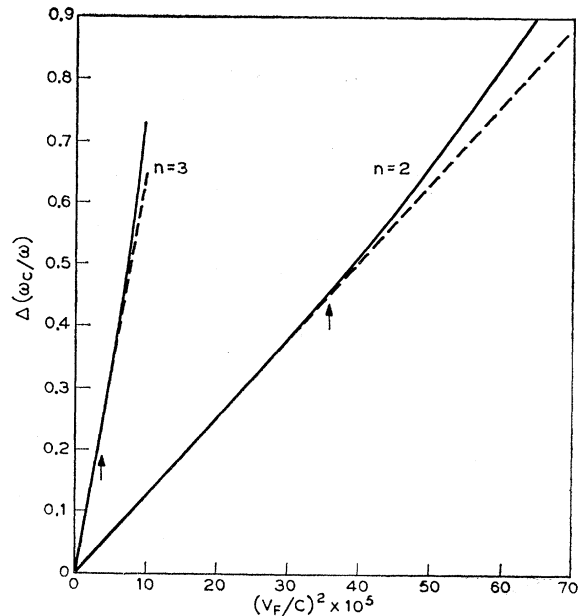


FIG. 5. Plot of the shift in position of the transmission maximum for the  $n=3$  and  $n=2$  geometric resonance as a function of  $(v_F/c)^2$  for fixed  $v_c/\omega = 0.01$  and  $\omega_p/\omega = 200$ .

parts of  $k$ , we find to lowest order in  $(v_F/c)^2$  that

$$\Delta\left(\frac{\omega_c}{\omega}\right) \approx \frac{1}{5} \left(\frac{\omega_p}{\omega}\right)^2 \left(\frac{v_F}{c}\right)^2 \frac{1}{(\omega_c/\omega - 1)^2}. \quad (29)$$

The subscript on the denominator in Eq. (29) indicates that it is to be evaluated at the resonance for zero temperature. The dependence of  $\Delta(\omega_c/\omega)$  on  $(v_F/c)$  is quadratic as anticipated. This *approximate* form for  $\Delta(\omega_c/\omega)$  is plotted on Fig. 5 as the dashed straight lines. The vertical arrows on this figure indicate those values of  $(v_F/c)$  for which  $|z|=1$ . We would expect the more accurate curves to deviate from the approximate curve in the neighborhood of the arrows. Indeed, this assumption is borne out.

In Fig. 6 are plots of the amplitude of the  $n=3$  and  $n=2$  transmission resonances for a fixed  $\nu_c/\omega=0.01$  as a function of  $(v_F/c)$ , and a fixed  $\omega_p/\omega=200$ . The decrease in amplitude cannot be computed using a power series expansion of the dielectric constant. This amplitude decrease is due to a resonance damping arising from that group of electrons which is traveling at the modified phase velocity of the disturbance in the plasma (see I). These electrons experience an effective static electric field. As a result they are accelerated in their orbit and spiral out around the lines of force. There is a net energy transfer from the wave to the electrons resulting in a damping of the wave. Mathematically, this resonance, or Landau, damping comes from the residue at the singularity in the denominator of Eq. (3) or, equivalently, the discontinuity across the branch cut in  $\epsilon(z,\omega)$  as  $z$  approaches the real axis for  $|z|>1$ . The arrows in Fig. 6 denote the condition  $|kv_F/(\omega_c - \omega)| = 1$ .

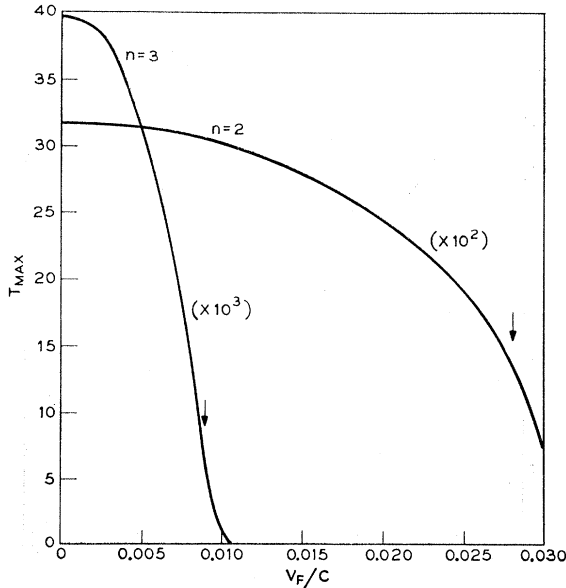


FIG. 6. Plot of the maximum amplitude of the  $n=3$  and  $n=2$  transmission resonance as a function of  $v_F/c$  for a fixed  $\nu_c/\omega=0.01$  and  $\omega_p/\omega=200$ .

If the disturbance in the plasma were accurately characterized by a single real wave number  $k$ , there would be no Landau damping present until the Fermi velocity became equal to the well-defined modified phase velocity  $|(\omega - \omega_c)/k|$ . On the basis of this rather crude argument, we would expect the curves in Fig. 6 to be flat to the left of the arrows. However, the finite collision frequency produces a small damping for all values of  $v_F/c$  and is thus responsible for the gradual change in slope of the curves in Fig. 6. To see that this is so we have plotted in Fig. 7 the amplitude of the  $n=3$  transmission resonance for an extremely small collision frequency,  $\nu_c/\omega=2 \times 10^{-5}$ , and an  $\omega_p/\omega=200$  as a function of  $v_F/c$ . The curve is nearly flat to the left of the arrow that denotes the condition  $|kv_F/(\omega_c - \omega)| = 1$  and falls off rapidly just to the right of it.

It is not obvious whether Landau damping in this problem represents true damping of the wave in the sense that the wave gives up energy to the plasma, or that it merely represents "phase mixing" so that no constructive interference can take place on successive reflections from the front and back surface. To answer this question, we have evaluated the net absorption by the slab,  $A=1-R-T$ , for two values of  $v_F/c$ , one to the left and one to right of the arrow in Fig. 7. The absorption  $A$  is plotted in Fig. 8 for  $\nu_c/\omega$  and  $\omega_p/\omega$  as given for Fig. 7. It can be seen that for  $v_F/c=0.0088$ , for which there is no Landau damping, the net absorption is small, while for  $v_F/c=0.0090$ , for which Landau damping is already present, an appreciable amount of energy is absorbed by the slab at resonance.

The decrease in amplitude of the resonance peaks depicted in Figs. 3 and 4 arises from Landau damping. However, in some respects the effect of this type of damping on the transmission resonances is different

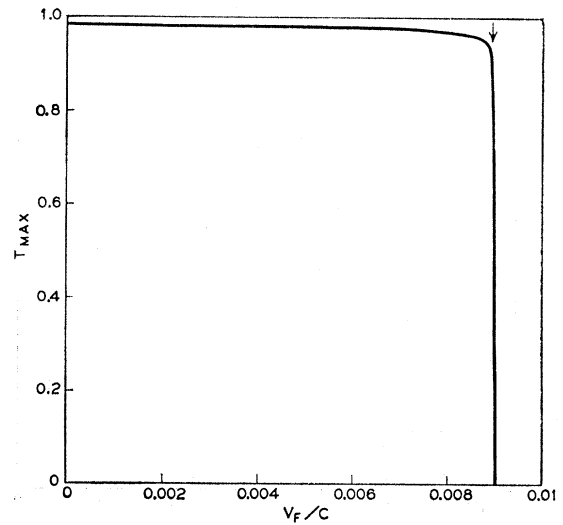


FIG. 7. Plot of the maximum amplitude of the  $n=3$  transmission resonance as a function of  $v_F/c$  for a fixed  $\nu_c/\omega=2 \times 10^{-5}$  and  $\omega_p/\omega=200$ .

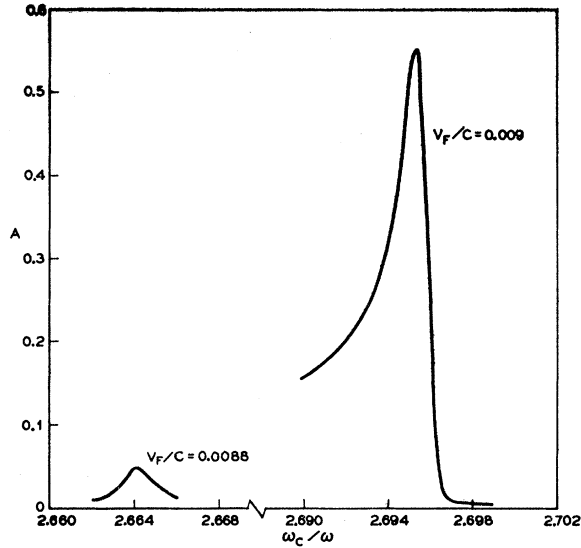


FIG. 8. Plot of the total power absorption ( $A=1-R-T$ , where  $R$  is the reflection coefficient) for the  $n=3$  transmission resonance as a function of magnetic field. The quantity  $v_e/\omega=2 \times 10^{-5}$  and  $\omega_p/\omega=200$ . The plots are made for two values of the Fermi velocity.

from the effect produced by a real short range collisional mechanism. There is practically no simultaneous broadening of the resonance with the decrease in amplitude. Only when the resonance has practically disappeared do the curves tend to broaden out.

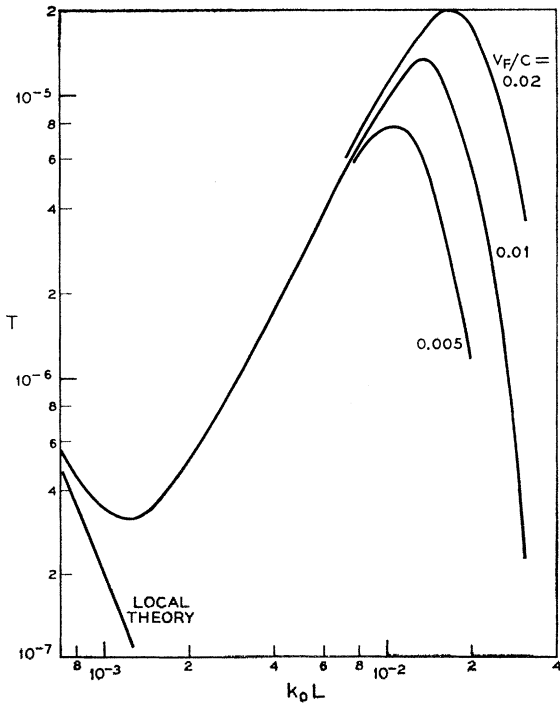


FIG. 9. Plot of the transmission coefficient  $T$  as a function of sample thickness  $L$  for fixed  $v_e/\omega=0.01$ ,  $\omega_p/\omega=200$ ,  $\omega_c/\omega=1.0$ , and several values of  $v_F/c$ .

### B. Field-Splash Effects

In the absence of nonlocal effects, for  $\omega_p/\omega \gg 1$  and for  $\omega_c/\omega < 1$ , the dielectric constant  $\epsilon(0, \omega)$  is large and negative and the wave in the medium is cut off. There will be no resonances of any kind in the transmitted power. The effect of finite temperature on the transmission characteristics is striking. Electrons moving with a finite velocity and traveling for distances of the order of a mean free path may carry field information deep into the plasma. The decay of the field and its subsequent transmission through the slab is limited not by the classical skin depth, but by mean free path effects (complete nonlocality). In fact, in I, it was shown that in a semi-infinite plasma the field, after an initial exponential decrease, may start to increase again at distances comparable to the wavelength of the disturbance inside the sample. In I, it was conjectured that this increase was due to a transfer of energy from the kinetic energy of the carriers to the electromagnetic field. This was so in a semi-infinite medium. However, for samples a few wavelengths (in the medium) thick, the presence of the second boundary should not appreciably affect the dependence of the field on distance. The field at the second boundary is much smaller than at the first, so that multiple reflection effects cannot be important. A plot of the transmission coefficient as a function of slab

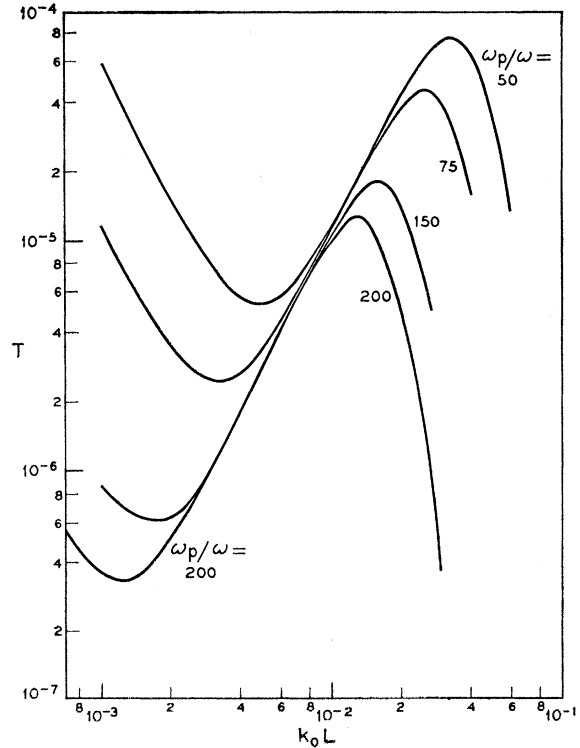


FIG. 10. Plot of the transmission coefficient  $T$  as a function of sample thickness  $L$  for fixed  $v_e/\omega=0.01$ ,  $v_F/c=0.01$ ,  $\omega_c/\omega=1.0$ , and for several values of  $\omega_p/\omega$ .

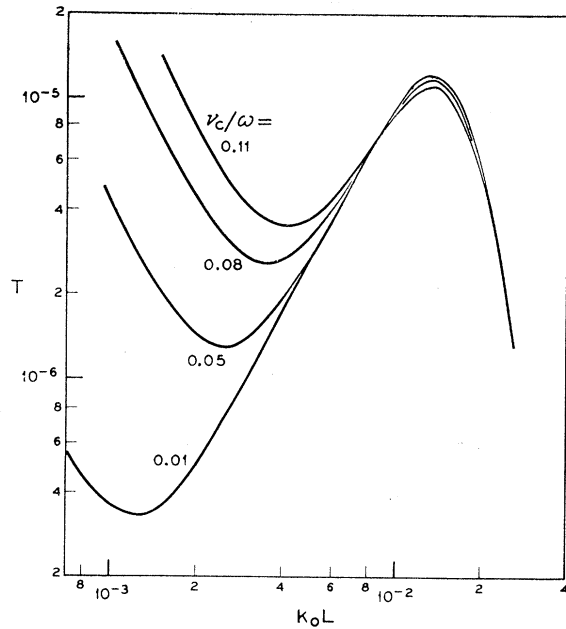


FIG. 11. Plot of the transmission coefficient  $T$  as a function of sample thickness  $L$  for fixed  $v_F/c=0.01$ ,  $\omega_p/\omega=200$ ,  $\omega_c/\omega=1.0$ , and for several values of  $\nu_c/\omega$ .

thickness should approximately trace out the dependence of the field on distance in the semi-infinite plasma.

We evaluated the transmission coefficient using Eqs. (15) and (20). Figures 9, 10, and 11 are plots of transmitted power as a function of slab thickness for various values of the electron gas parameters for a fixed  $\omega_c/\omega=1.0$ . In all cases the effect of temperature in the region of interest is to produce a single large "field-splash". The exponential decay of the transmitted power for small values of the slab thickness is characteristically followed by an exponential increase of one to

two orders of magnitude followed by an even sharper fall-off. The results of the local theory are plotted for comparison purposes in Fig. 9. At the point where the nonlocal theory predicts a maximum in the transmission, the transmission coefficient as computed from the local theory is seven to eight orders of magnitude smaller. In all cases that we considered, the minimum in the field splash occurs at a slab thickness approximately equal to one wavelength in the medium.

The effect of increasing  $v_F/c$  (Fig. 9) is to increase the magnitude of the effect, i.e., ratio of maximum to minimum, and to shift the position of the maximum only. To the left of the resonance, the curves for different  $v_F/c$  are extremely close to one another. The effect of decreasing  $(\omega_p/\omega)$  (Fig. 10), is to increase the splash very slightly and at the same time shift the curves as a whole to larger slab thicknesses and higher values of the transmission coefficient. The electron gas clearly becomes more transparent at lower plasma frequencies, hence, the increased value of the transmitted power. In addition, the wavelength in the medium increases with decreasing plasma frequency, therefore, the shift towards thicker slab dimensions of the minimum. No quantitative explanation of the shift of the maximum as a function of the parameters is offered since the existence of the maximum is probably due to a coherence effect.

The effect of increasing  $(\nu_c/\omega)$  (Fig. 11) is twofold. It decreases the magnitude of the effect and shifts the position of the minimum towards thicker samples, since the wavelength in the material at cyclotron resonance increases approximately as  $(\nu_c/\omega)^{1/2}$ .

#### ACKNOWLEDGMENT

The authors would like to thank Dr. E. I. Blount for his careful reading of the manuscript.